PHYSICAL REVIEW B VOLUME 34, NUMBER 8 15 OCTOBER 1986

Phonon scattering at electronically degenerate defect states: Theoretical approach and applications to acceptors in cubic semiconductors

Johannes Maier* and Ernst Sigmund
Institut für Theoretische Physik (Teil 3), Universität Stuttgart, Pfaffenwaldring 57/V,
D-7000 Stuttgart 80, Federal Republic of Germany

(Received 9 September 1985)

The specific (Jahn-Teller-type) electron-phonon interaction of electronically degenerate states leads to strong phonon scattering resonances in systems containing such defects, which are at some meV for acceptors in cubic semiconductors. Using a high-order Green-function calculation we show that these resonances are due to a dynamical splitting of the electronic degeneracy induced by thermal phonons. Application of an equation-of-motion technique gives a resonancelike formula for the scattering rate. We investigate the special case of an electronic Γ_8 state at acceptor defects in cubic semiconductors where these resonances were found in several experiments of various types in the last years. We discuss the physical properties of the resonance structures and the dependence on system parameters and compare with experimental results.

I. INTRODUCTION

In the last decade a series of new experimental techniques were developed which allow one to study very precisely phonon scattering and phonon transport properties of solids.[1] It was found that various kinds of lattice defects change these properties considerably,[2–5] and therefore the experimental interest focused on the behavior of such defect systems. Due to the high resolution of phonon experiments compared with optical studies, a new kind of resonance structure was found at electronically degenerate defect states, which could not be explained by direct transitions (direct resonances) between electronic levels.[2,5] The main features of these resonances are the extreme broad linewidth and the strong temperature dependence of the related phonon scattering rate, which is reflected in a considerable influence on thermal conductivity.[6] The first theoretical approach to explain the behavior of such systems was given several years ago by Rueff *et al.*[7] These authors used a model Hamiltonian of Jahn-Teller E-e-type which describes the coupling of a degenerate electronic two-level system with two degenerate vibrational modes of the lattice surroundings. Experimental evidence for these special phonon resonance structures came first from the study of weakly p-type doped cubic semiconductors like Si(In) or GaAs(Mn),[2,5] where a fourfold-degenerate electronic ground state (Γ_8 type) of the defect ions interact with nonsymmetric doubly degenerate (e) and triply degenerate (t) phonons of the lattice. This type of interaction is known as the Γ_8-$(e+t)$ Jahn-Teller (JT) case. This was the first evidence for the importance of the dynamic Jahn-Teller effect on the behavior of these semiconductor systems, which earlier had been considered as negligible due to the small coupling constants.[8]

The phonon scattering process at these electronically degenerate (JT) centers can be described as follows. Due to the coupling to nonsymmetric phonon modes the symmetry of the defect surrounding is lowered, leading to a dynamic splitting of the electronic multiplet. However, the coupled phonons play a twofold role. First they produce splittings in the electronic levels by means of thermally activated phonons. Owing to the absence of correlations and to the homogeneity of the heat bath these splittings are random and their temporal mean value vanishes.

Second, additional phonons can be scattered by the momentary electronic splittings. If these phonons are nonthermal a frequency-selective scattering rate will be observed. The effective resonance energy is related to the statistical distribution of these dynamical splittings.

In order to give an appropriate description of the dynamics of this phonon scattering process a high-order calculation is required to include the phonon-bath influences. Indeed perturbation theory in second-order Born approximation, which has so far been used for the calculation of the scattering process in these systems,[9] cannot account for these special phonon scattering resonances induced by the dynamic Jahn-Teller effect.

The theoretical approach of the present work is based on a Green-function method of high order, which allows an accurate description of the dynamic behavior of the electron-phonon interaction.

A complete theory of the frequency-dependent scattering rates, which are discussed in detail, is given. We used the results of this theory already in a previous paper[6] for the calculation of thermal conductivities. A Green-function treatment given earlier[10] led to a qualitative explanation of the resonance energies, but failed in the calculation of thermal conductivity line shapes.

In this paper we discuss the calculation of the relaxation rates within a Green-function approach via a T-matrix method. For the presentation here we present the formulas for the acceptor Γ_8 case. The approach is nevertheless common to all linear electron-phonon Hamiltonians. In a recent paper[11] we showed that donor defects can be described with a simplified version of the theory presented here.

II. SCATTERING THEORY

For the formulation of a scattering problem one usually starts with an eigenstate of an unperturbed Hamiltonian H_0, in which the whole Hamiltonian may be written as

$$H = H_0 + H_S \; . \tag{1}$$

If we take t_0 as a starting time the temporal evolution of an arbitrary state in interaction representation can formally be written as

$$\psi_I(t) = U(t,t_0)\psi_I(t_0) \; , \tag{2}$$

where the U matrix is defined by the integration procedure

$$U(t,t_0) = T_t \exp\left[-i \int_{t_0}^{t} H_I(t')dt' \right] \; . \tag{3}$$

T_t is the Dyson time-ordering operator and the index "I" denotes the interaction picture

$$\left[H_I(t) = \exp\left[-\frac{i}{\hbar} H_0 t \right] H_S \exp\left[+\frac{i}{\hbar} H_0 t \right] \right] \; .$$

Assuming that the perturbation is switched on adiabatically at $t_0 = -\infty$ and switched off adiabatically at $t = +\infty$ the initial (ϕ_a) and final (ψ_a) states are eigenstates to H_0. The final state after the scattering is given by

$$\psi_a = U(\infty, -\infty)\phi_a = S\phi_a \; . \tag{4}$$

Then for the time-dependent transition rate from an initial state ϕ_a to the final states ϕ_b one has

$$W_{b\text{-}a}(t) = |\langle \phi_b | [U(t,0) - 1] | \phi_a \rangle + \langle \phi_b | \phi_a \rangle |^2 \; , \tag{5}$$

where the second term contributes only for $a = b$ to the sum. With the definition of the T matrix[12]

$$\tilde{T} = \langle \phi_b | H_S | \psi_a \rangle \; , \tag{6}$$

the transition probability can be written as

$$P_{b\text{-}a} = \frac{d}{dt} W_{b\text{-}a}(t) = 2\pi |\tilde{T}_{ba}|^2 \delta(E_b - E_a) + 2\langle \phi_b | \phi_a \rangle \operatorname{Im} \tilde{T}_{ba} \; . \tag{7}$$

For the transition from a state a to all other states b one has therefore[12]

$$P_a = -2 \operatorname{Im} \tilde{T}_{aa} \; . \tag{8}$$

In the special case of a perturbed crystal P_a describes the transition from one phonon state to others onto the influence of the perturbation (e.g., electron-phonon coupling). The phonon states are characterized by a wave vector q and branch index λ. Then Eq. (8) reads for the relaxation rate of a phonon,

$$\tau_{q\lambda}^{-1} = P_{q\lambda} = -2 \operatorname{Im} \tilde{T}_{q\lambda,q\lambda} \; . \tag{9}$$

With the definition of the Green functions G_0 and G of the unperturbed (H_0) and perturbed (H) system as

$$G_0(\omega) = \frac{1}{\omega - H_0 + i\epsilon}, \quad G(\omega) = \frac{1}{\omega - H + i\epsilon} \; , \tag{10}$$

the T matrix can be calculated via a Dyson equation of the form[13]

$$G(\omega) = G_0(\omega) - G_0(\omega)\tilde{T}G_0(\omega) \; . \tag{11}$$

Therefore the determination of the relaxation rate [Eq. (9)] is reduced to the calculation of the Green functions of the crystal. As discussed before, in order to be able to describe the dynamic scattering mechanism at the JT defects in the calculations, we have to go far beyond the usual second-order Born approximation. Therefore we have to perform a high-order calculation of the phonon-phonon Green functions of the perturbed system. In our paper this will be done by the equation-of-motion method by which a natural hierarchy in orders of the perturbation parameter appears.[14]

III. DEFECT HAMILTONIAN

The Hamiltonian we will deal with in this paper contains linear electron-phonon interaction terms of localized electronic states with lattice coordinates. It can be written in the general form as

$$H = \sum_{q,\lambda} \omega_{q\lambda} b_{q\lambda}^{\dagger} b_{q\lambda} + \sum_{q,\lambda} \Lambda^{q\lambda} Q_{q\lambda} \; , \tag{12}$$

where $Q^{q\lambda}$ are the phonon coordinates defined by the phonon creation and annihilation operators for wave vector q and branch index λ,

$$Q_{q\lambda} = b_{q\lambda} + b_{q\lambda}^{\dagger} \tag{13}$$

and $\Lambda^{q\lambda}$ are bilinear in the electronic operators of the defect state, the special form of which depends on the electronic symmetry structure.

For further use in this work we will specialize Eq. (12) for acceptor defects in cubic semiconductors, which can be described by the effective-mass approximation (EMA). Examples for such systems are Si(In), Si(B), GaAs(Mn), etc. The symmetry of the acceptor ground state which is determined by the Γ point of the valence band is Γ_8; it is fourfold degenerate. From group-theoretical arguments the electrons may interact with e- and t-type phonons only [$\Gamma_8 - (e_g + t_{2_g})$ JT case].

The four degenerate electronic levels can be described by operators which can be classified according to the 15 generators of the SU(4) Lie algebra. These 15 generators may be represented with the help of two independent spin algebras $\{\rho_j\}$ and $\{\sigma_j\}$ with commutation relations[15]

$$\begin{aligned} &[\rho_i, \rho_j] = 2i\epsilon_{ijk}\rho_k, \quad [\sigma_i, \sigma_j] = 2i\epsilon_{ijk}\sigma_k \; , \\ &[\sigma_i, \rho_k] = 0 \; . \end{aligned} \tag{14}$$

Their definition within the electronic operators is given in Appendix A. As we will see later, these simple spin commutation relations are very convenient for the Green-function's expansion.

Taking only the fourfold degenerate acceptor ground state and its interaction with the lattice vibrations into account, the total Hamiltonian of the considered semiconductor systems then reads

$$H=\omega_\epsilon \sum_{j=1}^{2} b^\dagger_{\Gamma_{3,j}} b_{\Gamma_{3,j}} + \omega_\tau \sum_{k=1}^{3} b^\dagger_{\Gamma_{5,k}} b_{\Gamma_{5,k}} + K_\epsilon \sum_{j=1}^{2} \rho_j (b^\dagger_{\Gamma_{3,j}} + b_{\Gamma_{3,j}}) + K_\tau \rho_3 \sum_{k=1}^{3} \sigma_k (b^\dagger_{\Gamma_{5,k}} + b_{\Gamma_{5,k}}) \ . \tag{15}$$

Here j and k are indices each of which describes the wave vector q and branch λ. Γ_3 is symbol for the group-theoretical representation of the twofold degenerate (e) and Γ_5 of the threefold degenerate (t) phonon modes. ω_ϵ and ω_τ are the phonon frequencies, K_ϵ and K_τ are the two independent coupling constants, which depend in general on q and λ. Expressing the symmetry coordinates of the Γ_3 and Γ_5 vibrations of the defect as projections from the lattice phonons we end up with the interaction Hamiltonian of the form

$$H_{e\text{-ph}}=\sum_{q,\lambda} \left[D_\epsilon \sum_{j=1}^{2} \rho_i r_i^{q\lambda} + D_\tau \rho_3 \sum_{k=1}^{3} \sigma_k s_k^{q\lambda} \right] (b_{q\lambda} + b^\dagger_{q\lambda}) \ , \tag{16}$$

where the projectors $r_i^{q\lambda}$ and $s_i^{q\lambda}$ are defined as

$$r_1^{q\lambda}=\alpha(q) f(q) \tfrac{1}{3} (2\hat{q}_z n_{\lambda z} - \hat{q}_x n_{\lambda x} - \hat{q}_y n_{\lambda y}) \ , \tag{17a}$$

$$r_2^{q\lambda}=\alpha(q) f(q) \frac{1}{\sqrt{3}} (\hat{q}_x n_{\lambda x} - \hat{q}_y n_{\lambda y}) \ , \tag{17b}$$

$$s_1^{q\lambda}=\alpha(q) f(q) \frac{1}{\sqrt{3}} (\hat{q}_z n_{\lambda y} + \hat{q}_y n_{\lambda z}) \ , \tag{17c}$$

$$s_2^{q\lambda}=\alpha(q) f(q) \frac{1}{\sqrt{3}} (\hat{q}_z n_{\lambda x} + \hat{q}_x n_{\lambda z}) \ , \tag{17d}$$

$$s_3^{q\lambda}=\alpha(q) f(q) \frac{1}{\sqrt{3}} (\hat{q}_x n_{\lambda y} + \hat{q}_y n_{\lambda x}) \ , \tag{17e}$$

with the abbreviations $(i=x,y,z)$: $\hat{q}_i = q_i / |\mathbf{q}|$ and

$$\alpha(q) = \left[\frac{\hbar \omega_{q\lambda}}{2Mc_\lambda^2} \right]^{1/2} \ . \tag{18}$$

M is the mass of the crystal, $\omega_{q\lambda}$ the phonon frequency, and c_λ $(\lambda = l,t)$ the sound velocity of the longitudinal (l) and transverse (t) modes. $n_{\lambda i}$ are polarization vectors. $f(q)$ describes the extension of the defect which leads to a cutoff for small phonon wavelengths. The most simple treatment of this cutoff function is within the effective-mass approximation,[16] where the acceptor wave functions are determined by a hydrogenlike model. Considering only the s-like parts of the acceptor ground state, $f(q)$ reads

$$f(q) = [1 + \tfrac{1}{4} (a^*)^2 q^2]^{-2} \ , \tag{19}$$

where a^* is the so-called Bohr radius of the defect, i.e., a measure of the extension of the defect wave function. Defining

$$\eta_{1,2}^{q\lambda} = r_{1,2}^{q\lambda}, \quad \eta_{3,4,5}^{q\lambda} = s_{1,2,3}^{q\lambda} \ , \tag{20a}$$

$$\xi_{1,2} = \rho_{1,2}, \quad \xi_{3,4,5} = \rho_3 \sigma_{1,2,3} \ , \tag{20b}$$

one gets the abbreviations

$$\Lambda^{q\lambda} = \sum_{i=1}^{5} \xi_i \eta_i^{q\lambda}, \quad H_{e\text{-ph}} = \sum_{q,\lambda} \Lambda^{q\lambda} Q_{q\lambda} \ , \tag{21}$$

together with the diagonal part of the phonons the general structure of Eq. (12). In the following we will use this general form for our Green-function calculations.

IV. GREEN FUNCTIONS AND THE ONE-MODE RELAXATION RATE

For the calculation the method of thermodynamical Green functions is used.[14] The retarded Green function for two arbitrary operators $\hat{A}$ and $\hat{B}$ is defined by

$$G^r(t,t') = \langle\langle \hat{A}(t); \hat{B}(t') \rangle\rangle^r_\eta = -i\Theta(t-t') \langle [\hat{A}(t), \hat{B}(t')]_\eta \rangle_T \ . \tag{22}$$

$\eta = 1$ denotes the commutator and $\eta = -1$ the anticommutator. In our case we have $\eta = 1$.

$\Theta(t)$ is the Heaviside function and $\langle \cdots \rangle_T$ the thermal expectation value,

$$\langle \hat{A} \rangle_T = \mathrm{Tr}(e^{-\beta H} \hat{A}) / \mathrm{tr}(e^{-\beta H}) \ . \tag{23}$$

The equation of motion in Fourier space is given in the form

$$\omega \langle\langle \hat{A}; \hat{B} \rangle\rangle_\omega = \frac{1}{2\pi} \langle [\hat{A}, \hat{B}]_T + \langle\langle [\hat{A}, H]; \hat{B} \rangle\rangle_\omega = \frac{1}{2\pi} \langle [\hat{A}, \hat{B}] \rangle_T - \langle\langle \hat{A}; [\hat{B}, H] \rangle\rangle_\omega \tag{24}$$

by which a Green function is expressed by another "higher" one and therefore a hierarchy is built up.

In nontrivial cases this hierarchy cannot be closed exactly and therefore approximations have to be made. However, there are some exact relations for these Green functions,[14] which allow one to check the approximations

$$\langle\langle \hat{B}; \hat{A} \rangle\rangle = \langle\langle \hat{A}; \hat{B} \rangle\rangle_{-\omega} \ , \tag{25}$$

$$\int_{-\infty}^{\infty} \langle\langle \hat{A}; \hat{B} \rangle\rangle d\omega = -\pi \langle [\hat{A}, \hat{B}] \rangle_T \ , \tag{26}$$

$$\int_{-\infty}^{\infty} (\omega \langle\langle \hat{A}; \hat{B} \rangle\rangle - \langle [\hat{A}, \hat{B}] \rangle_T) d\omega = \pi \left\langle \left[\frac{\partial \hat{A}}{\partial t}, \hat{B} \right] \right\rangle_T^{t=0} \ . \tag{27}$$

In the following we will use this method to calculate the phonon scattering mechanism in defect systems with electronically degenerate levels, where we concentrate on the previously mentioned semiconductor examples. As already stated, for the physical nature of the phonon scattering resonances at these electronically degenerate systems, the following simplified picture can be constructed.

According to the JT theorem the interaction with the degenerate crystal phonons lowers the electronic symmetry and creates dynamical splittings of the degenerate electronic levels. However, due to all the different thermal crystal phonons the thermal average over the ion displacements Q vanishes and therefore no static splittings can be seen. Nevertheless there are fluctuating splittings and an additional phonon can be scattered at such a momentary split electronic level. From this simplified picture one can draw some important conclusions, namely, the coupling of the whole phonon bath splitting is expected to be strongly temperature dependent and the fluctuations of the splittings of the resonances will be very broad. Both of these features are observed in experiments.[3-5]

As pointed out already for theoretical considerations the nature of these resonances implies a high-order theory to describe the phenomena. According to Eqs. (9) and (11) for the calculation of the relaxation rate we start with the lattice (phonon-phonon) Green function which is defined by[17,18]

$$G_{q\lambda,q'\lambda'}(\omega)=-\pi(\omega_{q\lambda}\omega_{q'\lambda'})^{-1/2} \times \langle\langle b_{q\lambda}+b^{\dagger}_{q\lambda};b_{q'\lambda'}+b^{\dagger}_{q'\lambda'}\rangle\rangle \ . \tag{28}$$

For the unperturbed crystal ($H=H_0$) the Green-function hierarchy is closed in second order and we get

$$G_{0_{q\lambda,q'\lambda'}}(\omega)=\frac{\delta_{qq'}\delta_{\lambda\lambda'}}{\omega^2-\omega^2_{q\lambda}} \ . \tag{29}$$

In the case of the perturbed system ($H=H_0+H_s$) one gets after a simple application of (24) the exact relation

$$\langle\langle b_{q\lambda}+b^{\dagger}_{q\lambda};b_{q'\lambda'}+b^{\dagger}_{q'\lambda'}\rangle\rangle=\frac{\omega_{q\lambda}\delta_{qq'}\delta_{\lambda\lambda'}}{\pi(\omega^2-\omega^2_{q\lambda})}+\frac{4\omega_{q\lambda}\omega_{q'\lambda'}}{(\omega^2-\omega^2_{q\lambda})(\omega^2-\omega^2_{q'\lambda'})} \times\langle\langle \Lambda^{q\lambda};\Lambda^{q'\lambda'}\rangle\rangle \ . \tag{30}$$

Comparison with Eq. (11) yields for the relaxation rate

$$\tau^{-1}_{q\lambda}=4\pi_n V\,\mathrm{Im}\langle\langle \Lambda^{q\lambda};\Lambda^{q\lambda}\rangle\rangle \ , \tag{31}$$

where n is the defect concentration and V is the crystal volume. $\Lambda^{q\lambda}$ is the pure electronic part of the interaction Hamiltonian and therefore instead of a phonon-phonon Green function we are left the calculation of spin-spin Green functions. For the mean relaxation time of branch λ and frequency ω the following relation holds:

$$\langle \tau^{-1}_{\lambda}(\omega)\rangle=\frac{\sum\limits_{q}\tau^{-1}_{q\lambda}\delta(\omega_{q\lambda}-\omega)}{\sum\limits_{q,\lambda}\delta(\omega_{q\lambda}-\omega)} \ . \tag{32}$$

Inserting Eq. (32) into Eq. (31) using a Debye model for the phonons and performing the sum over q into an integral leads us to

$$\langle \tau^{-1}_{\lambda}(\omega)\rangle=n\frac{\hbar\omega f^2_{\lambda}(\omega)\bar{c}^{\,3}}{2\rho c^5_{\lambda}}\sum_{i}A^{\lambda}_{i}\mathrm{Im}\langle\langle \xi_j;\xi_j\rangle\rangle \ , \tag{33}$$

where

$$\bar{c}^{\,3}=\left[\sum_{\lambda}\frac{1}{c^3_{\lambda}}\right]^{-1}$$

and

$$f_{\lambda}(\omega)=\left[1+\frac{(a^*)^2\omega^2}{4c^2_{\lambda}}\right]^{-2} .$$

The A^{λ}_{j} result from the angle-dependent integration and are given in Appendix B. According to the interaction Hamiltonian for the calculation of the relaxation rate only five independent "diagonal" Green functions $\langle\langle \xi_j;\xi_j\rangle\rangle$ are necessary.

V. GREEN-FUNCTION HIERARCHY

For the evaluation of the Green functions we start with the following hierarchy of equations:

$$\omega\langle\langle \xi_1;\xi_1\rangle\rangle=\sum_{q,\lambda}\langle\langle Q[\xi_1,\Lambda];\xi_1\rangle\rangle \ , \tag{34}$$

where $Q^{q\lambda}$ is simplified to Q, the same applies to Λ. The following higher Green functions read:

$$\omega\langle\langle Q[\xi_1,\Lambda];\xi_1\rangle\rangle=\frac{1}{2\pi}\langle Q[[\xi_1,\Lambda],\xi_1]\rangle_T+\omega_{q\lambda}\langle\langle P[\xi_1,\Lambda];\xi_1\rangle\rangle+\sum_{q',\lambda'}\langle\langle QQ'[[\xi_1,\Lambda],\Lambda'];\xi_1\rangle\rangle \tag{35}$$

and

$$\omega\langle\langle P[\xi_1,\Lambda];\xi_1\rangle\rangle=\frac{1}{2\pi}\langle P[[\xi_1,\Lambda],\xi_1]\rangle_T+2\langle\langle \Lambda[\xi_1,\Lambda];\xi_1\rangle\rangle+\omega_{q\lambda}\langle\langle Q[\xi_1,\Lambda];\xi_1\rangle\rangle+\sum_{q',\lambda'}\langle\langle PQ'[[\xi_1,\Lambda],\Lambda'];\xi_1\rangle\rangle \ . \tag{36}$$

This hierarchy of one-phonon operators can be closed exactly and yields

$$(\omega^2-\omega^2_{q\lambda})\langle\langle Q[\xi_1,\Lambda];\xi_1\rangle\rangle=\frac{\omega}{2\pi}\langle Q[[\xi_1,\Lambda],\xi_1]\rangle_T+\frac{\omega_{q\lambda}}{2\pi}\langle P[[\xi_1,\Lambda],\xi_1]\rangle_T+\omega\sum_{q',\lambda'}\langle\langle QQ'[[\xi_1,\Lambda],\Lambda'];\xi_1\rangle\rangle +\omega_{q\lambda}\sum_{q',\lambda'}\langle\langle PQ'[[\xi_1,\Lambda],\Lambda'];\xi_1\rangle\rangle+2\omega_{q\lambda}\langle\langle \Lambda[\xi_1,\Lambda];\xi_1\rangle\rangle \ . \tag{37}$$

Three new Green functions appear on the right-hand side. For the first one a random-phase-approximation (RPA) factorization yields

$$\langle\langle QQ'[[\xi_1,\Lambda],\Lambda'];\xi_1\rangle\rangle \approx \langle QQ'\rangle_T \hat{P}([[\xi_1,\Lambda],\Lambda'] \rightarrow \xi_1)\langle\langle \xi_1;\xi_1\rangle\rangle \ , \tag{38}$$

where $\hat{P}(e \rightarrow \xi_i)$ denotes the projection on the electronic operator ξ_i. With Eq. (38) the first Green function on the right-hand side of Eq. (37) is closed to the original Green function in (34). The phonon part in the second function of Eq. (37) does not commute with the unperturbed Hamiltonian (H_0). The next equation of motion therefore yields terms of the same order,

$$\begin{aligned}\omega\langle\langle PQ'[[\xi_1,\Lambda],\Lambda'];\xi_1\rangle\rangle = {} & \frac{1}{2\pi}\langle PQ'([[\xi_1,\Lambda],\Lambda'],\xi_1)\rangle_T + \omega_{q\lambda}\langle\langle QQ'[[\xi_1;\Lambda],\Lambda'];\xi_1\rangle\rangle \\ & + \omega_{q'\lambda'}\langle\langle PP'[[\xi_1,\Lambda],\Lambda'];\xi_1\rangle\rangle + \sum_{q'',\lambda''}\langle\langle PQ'Q''([[\xi_1,\Lambda],\Lambda'],\Lambda'');\xi_1\rangle\rangle \\ & + 2\langle\langle Q'\Lambda[[\xi_1,\Lambda],\Lambda'];\xi_1\rangle\rangle \ ,\end{aligned} \tag{39}$$

where the functions with PP' and QQ' can be closed along Eq. (38). The higher electronic Green function of Eq. (37) is expanded to yield

$$\omega\langle\langle \Lambda[\xi_1,\Lambda];\xi_1\rangle\rangle = \frac{1}{2\pi}\langle[\Lambda[\xi_1,\Lambda],\xi_1]\rangle_T + \sum_{q'',\lambda''}\langle\langle Q''[\Lambda[\xi_1,\Lambda],\Lambda''];\xi_1\rangle\rangle \ . \tag{40}$$

The remaining Green function all have odd numbers of phonon operators. Therefore no RPA procedure in phonon space can be applied.

According to Eq. (8) the result for the relaxation rate has to be of positive definiteness. A shortcoming of the expansion method here is the fact that approximations which are not accurate enough usually distort this physical property. In order to get reasonable results we demand positive definiteness together with the validity of Eqs. (25)–(27).

Before starting with an approximation scheme of the higher functions we write down the various expectation values appearing in the Green-function's expansion and which are given already in Ref. 6. They are exact up to $O(K^2)$ ($\hbar=1$)

$$\langle QQ'\rangle_T = \delta_{qq'}\delta_{\lambda\lambda'}\coth\left[\frac{\omega_{q\lambda}}{2k_BT}\right] + \frac{4}{\omega_{q\lambda}\omega_{q'\lambda'}}\sum_{i=1}^{5}\eta_i^{q\lambda}\eta_i^{q'\lambda'} + \cdots \ ,$$

$$\langle Q\xi_j\rangle_T = \begin{cases} -\dfrac{2}{\omega_{q\lambda}}\eta_j^{q\lambda}, & j=1,2,\cdots 5 \\ 0, & j>5 \end{cases}$$

$$\langle P\xi_j\rangle_T = 0 \ ,$$

$$\langle PP'\rangle_T = -\delta_{qq'}\delta_{\lambda\lambda'}\coth(\omega_{q\lambda}/2k_BT)$$

(k_B = Boltzmann factor).

For the remaining Green functions we get the following.

(i) $\langle\langle Q'\Lambda[[\xi_1,\Lambda],\Lambda'];\xi_1\rangle\rangle$ which contains one exact closing part

$$\langle\langle Q'\Lambda[[\xi_1,\Lambda],\Lambda'];\xi_1\rangle\rangle = -4\sum_{j\,(\neq 1)}\eta_j\eta_j\eta_1'\langle\langle Q';\xi_1\rangle\rangle \ . \tag{41}$$

Together with

$$\langle\langle Q';\xi_1\rangle\rangle = 2\frac{\omega_{q'\lambda'}}{\omega^2-\omega_{q'\lambda'}^2}\langle\langle \Lambda';\xi_1\rangle\rangle \ , \tag{42}$$

the exact reconstruction of the original function reads as

$$-8\left[\sum_{j\,(\neq 1)}\eta_j\eta_j\right]\eta_1'\eta_1'\frac{\omega_{q'\lambda'}}{\omega^2-\omega_{q'\lambda'^2}}\langle\langle \xi_1;\xi_1\rangle\rangle \ . \tag{43}$$

The remaining parts are dealt together with the following function.

(ii) $\langle\langle Q'[\Lambda[\xi_1,\Lambda],\Lambda'];\xi_1\rangle\rangle$ and with the abbreviation E for an arbitrary electronic operator one has

$$\begin{aligned}(\omega^2-\omega_{q'\lambda'}^2)\langle\langle Q'E;\xi_1\rangle\rangle = {} & \omega\left[\langle Q'[E,\xi_1]\rangle_T + \sum_{q'',\lambda''}\langle\langle Q'Q''[E,\Lambda''];\xi_1\rangle\rangle\right] \\ & + \omega_{q\lambda'}\left[\langle P'[E,\xi_1]\rangle_T + \sum_{q'',\lambda''}\langle\langle P'Q''[E,\Lambda''];\xi_1\rangle\rangle + 2\langle\langle \Lambda'E;\xi_1\rangle\rangle\right] \ .\end{aligned} \tag{44}$$

Only the last term closes the hierarchy. Together with (43) one obtains

$$\begin{aligned}& 2\omega_{q\lambda}\sum_{q',\lambda'}(\langle\langle Q'[\Lambda[\xi_1,\Lambda],\Lambda'];\xi_1\rangle\rangle + \langle\langle Q'\Lambda[[\xi_1,\Lambda],\Lambda'];\xi_1\rangle\rangle) \\ & \qquad = \left[-32\left[\sum_{j\,(\neq 1)}\eta_j\eta_j\right]\eta_1'\eta_1' + 16\left[\sum_{m\,(\neq 1)}\eta_m\eta_m\eta_m'\eta_m'\right]\right]\frac{\omega_{q\lambda}\omega_{q'\lambda'}}{\omega^2-\omega_{q'\lambda'}^2}\langle\langle \xi_1;\xi_1\rangle\rangle \ .\end{aligned} \tag{45}$$

(iii) $\langle\langle PQ'Q''[[[\xi_1,\Lambda],\Lambda'],\Lambda''];\xi_1\rangle\rangle$ expansion gives

$$\begin{aligned}\langle\langle PQ'Q''[[[\xi_1,\Lambda],\Lambda'],\Lambda''];\xi_1\rangle\rangle \approx 16\Bigg[&\frac{1}{\omega_{q''\lambda''}}\left[\sum_{i\,(\neq 1)}\eta_i\eta_i\right]\left[\sum_{k\,(\neq 1)}\eta''_k\eta''_k\right]\delta_{qq'}\delta_{\lambda\lambda'}\\ &+\frac{1}{\omega_{q'\lambda'}}\sum_{l\,(\neq 1)}\eta_l\eta_l\eta'_l\eta'_l\delta_{qq''}\delta_{\lambda\lambda''}\\ &-\delta_{q'q''}\delta_{\lambda'\lambda''}\frac{1}{\omega_{q\lambda}}\coth\left[\frac{\beta\omega_{q\lambda}}{2}\right]\coth\left[\frac{\beta\omega_{q'\lambda'}}{2}\right]\\ &\times\left[\sum_{l\,(\neq 1)}\eta_l\eta_l\eta'_l\eta'_l+\eta'_1\eta'_1\sum_{j\,(\neq 1)}\eta_j\eta_j\right]\Bigg]\langle\langle\xi_1;\xi_1\rangle\rangle\ . \end{aligned} \tag{46}$$

Now the closure is completed.

The next step is to calculate the remaining q summations in the Green-function expressions. This can be done by converting the summations into integrations,

$$\sum_q \eta_i^{q\lambda}\eta_j^{q\lambda}\cdots=\delta_{ij}A_j^\lambda\gamma_\lambda\int_0^{\omega_D}d\omega_{q\lambda}\,\omega_{q\lambda}^3 f_\lambda^2(\omega_{q\lambda})\cdots\ , \tag{47}$$

where

$$\gamma_\lambda=\frac{1}{(2\pi)^3}\frac{\hbar}{2\rho c_\lambda^5}\ .$$

The resonance terms within the integral are converted into Cauchy-type integrals with the common relation[7]

$$\int dx\frac{1}{a-x}f(x)=i\pi f(a)+\mathrm{P}\left[\int dx\frac{1}{a-x}f(x)\right]\ . \tag{48}$$

For the resulting integrals the following abbreviations are chosen:

$$\tilde{S}^\lambda(\omega,n)\equiv\mathrm{P}\left[\int_0^{\omega_D}d\omega_{q\lambda}f_\lambda^2(\omega_{q\lambda})\right]\frac{\omega_{q\lambda}^n\coth\left[\dfrac{\beta\omega_{q\lambda}}{2}\right]}{\omega^2-\omega_{q\lambda}^2}\ , \tag{49a}$$

$$S^\lambda(\omega,n)\equiv\mathrm{P}\left[\int_0^{\omega_D}d\omega_{q\lambda}f_\lambda^2(\omega_{q\lambda})\right]\frac{\omega_{q\lambda}^n}{\omega^2-\omega_{q\lambda}^2}\ , \tag{49b}$$

$$R^\lambda(n)\equiv\int_0^{\omega_D}d\omega_{q\lambda}f_\lambda^2(\omega_{q\lambda})\omega_{q\lambda}^n\ , \tag{49c}$$

$$\tilde{R}^\lambda(n)\equiv\int_0^{\omega_D}d\omega_{q\lambda}f_\lambda^2(\omega_{q\lambda})\omega_{q\lambda}^n\coth\left[\frac{\beta\omega_{q\lambda}}{2}\right]\ . \tag{49d}$$

The analytical calculation is given in Appendix C.

VI. PHONON RELAXATION RATE

As a final result we get a Lorentzianlike expression for the phonon relaxation rate (32)

$$\langle\tau^{-1}(\omega)\rangle=\frac{8}{9}(D_e)^2\frac{\hbar\omega n\pi}{\rho\bar{c}^2}\frac{1}{9}\times\sum_{\lambda=1}^{3}f_\lambda^2(\omega)\frac{[\omega^2-\Delta(\omega)]\beta(\omega)-\alpha(\omega)\Gamma(\omega)}{[\omega^2-\Delta(\omega)]^2+\Gamma(\omega)^2}\ . \tag{50}$$

Here we used the following abbreviations. With the definitions

$$T_\lambda\equiv\sum_{i(\neq 1)}A_i^\lambda,\quad T_{2\lambda}\equiv\sum_{i,j}A_i^\lambda A_j^\lambda,\quad i\neq j,\quad i\neq 1,\quad j\neq 1$$

$$T_{3\lambda\lambda'}\equiv\sum_{j\,(\neq 1)}A_j^\lambda A_j^{\lambda'},\quad T_{4\lambda\lambda'\lambda''}\equiv\sum_{k\,(\neq 1)}A_k^\lambda A_k^{\lambda'}A_k^{\lambda''}\ ,$$

and

$$U_{\lambda\lambda'}\equiv-(T_{\lambda'}T_{\lambda'}+2T_{3\lambda\lambda'})\ ,$$

$$X_{\lambda\lambda'}\equiv 2T_\lambda A_1^{\lambda'}-T_{3\lambda\lambda'}\ ,$$

$$W_{\lambda\lambda'}\equiv T_{3\lambda\lambda'}+T_{\lambda'}A_1^{\lambda'}\ ,$$

$$Y_{\lambda\lambda'}\equiv 3T_{3\lambda\lambda'}+T_\lambda T_{\lambda'}\ ,$$

together with

$$\delta_\lambda\equiv(4\pi^2\rho c_\lambda^5\hbar^2k_B)^{-1}\ .$$

The functions appearing in (50) read as

$$\alpha(\omega)=\frac{4\hbar\omega^2}{\pi}\sum_\lambda\delta_\lambda S'(\omega,2)[T_\lambda+16\delta_\lambda\hbar T_{2\lambda}\tilde{R}^\lambda(1)]\ , \tag{51}$$

$$\beta(\omega)=2\hbar^2\omega^3\sum_\lambda\delta_\lambda f_\lambda^2(\omega)[T_\lambda+16\delta_\lambda\hbar T_{2\lambda}\tilde{R}^\lambda(1)]\ , \tag{52}$$

$$\Delta(\omega)=-\sum_{i=1}^{6}\Delta_i(\omega)\ , \tag{53}$$

$$\Gamma(\omega)=-\sum_{i=1}^{5}\Gamma_i(\omega)\ , \tag{54}$$

and

$$\Delta_1(\omega)=4(\hbar\omega)^2\sum_\lambda\delta_\lambda T_\lambda\tilde{S}^\lambda(\omega,3)\ , \tag{53a}$$

$$\Delta_2(\omega)=16\omega^2\sum_{\lambda,\lambda'}\delta_\lambda\delta_{\lambda'}S^\lambda(\omega,2)R^{\lambda'}(2)T_{3\lambda\lambda'}\ , \tag{53b}$$

$$\Delta_3(\omega)=\frac{16}{\hbar^2}\sum_{\lambda,\lambda'}\delta_\lambda\delta_{\lambda'}S^\lambda(\omega,4)[R^{\lambda'}(2)U_{\lambda\lambda'}+S^{\lambda'}(\omega,4)X_{\lambda\lambda'}]\ , \tag{53c}$$

$$\Delta_4(\omega)=4\pi^2\hbar^4\omega^6\sum_{\lambda,\lambda'}\delta_\lambda\delta_{\lambda'}f_\lambda^2(\omega)f_{\lambda'}^2(\omega)X_{\lambda\lambda'}\ , \tag{53d}$$

$$\Delta_5(\omega)=-16\hbar^3\sum_{\lambda,\lambda'}\delta_\lambda\delta_{\lambda'}\widetilde{S}^{\lambda}(\omega,3)\widetilde{R}^{\lambda'}(3)W_{\lambda\lambda'}\ , \tag{53e}$$

$$\Delta_6(\omega)=-\frac{64}{\hbar^2}\sum_{\lambda,\lambda',\lambda''}\delta_\lambda\delta_{\lambda'}\delta_{\lambda''}\widetilde{S}^{\lambda}(\omega,3)R^{\lambda'}(2)R^{\lambda''}(2)$$

$$\times(T_\lambda A_1^{\lambda'}A_1^{\lambda''}+T_{4\lambda\lambda'\lambda''})\ , \tag{53f}$$

$$\Gamma_1(\omega)=\pi\hbar^2\omega^4\coth\left[\frac{\beta\omega}{2}\right]\sum_{\lambda}\delta_\lambda f_\lambda^2(\omega)T_\lambda\ , \tag{54a}$$

$$\Gamma_2(\omega)=-16\hbar\omega^3\sum_{\lambda,\lambda'}\delta_\lambda\delta_{\lambda'}f_\lambda^2(\omega)S^{\lambda'}(\omega,4)X_{\lambda\lambda'}\ , \tag{54b}$$

$$\Gamma_3(\omega)=8\hbar\omega^3\pi\sum_{\lambda,\lambda'}\delta_\lambda\delta_{\lambda''}f_\lambda^2(\omega)R^{\lambda}(2)Y_{\lambda\lambda'}\ , \tag{54c}$$

$$\Gamma_4(\omega)=-8\hbar^4\omega^2\coth\left[\frac{\beta\omega}{2}\right]\pi\sum_{\lambda,\lambda'}\delta_\lambda\delta_{\lambda'}\widetilde{R}^{\lambda}(3)W_{\lambda\lambda'}\ , \tag{54d}$$

$$\Gamma_5(\omega)=-\frac{32\pi}{\hbar}\omega^2\coth\left[\frac{\beta\omega}{2}\right]$$

$$\times\sum_{\lambda,\lambda',\lambda''}\delta_\lambda\delta_{\lambda'}\delta_{\lambda''}f_\lambda^2(\omega)R^{\lambda}(2)$$

$$\times(T_\lambda A_1^{\lambda'}A_1^{\lambda''}+T_{4\lambda\lambda'\lambda''})\ . \tag{54e}$$

To be in accordance with the denominator, the thermal expectation values were expanded to higher orders.

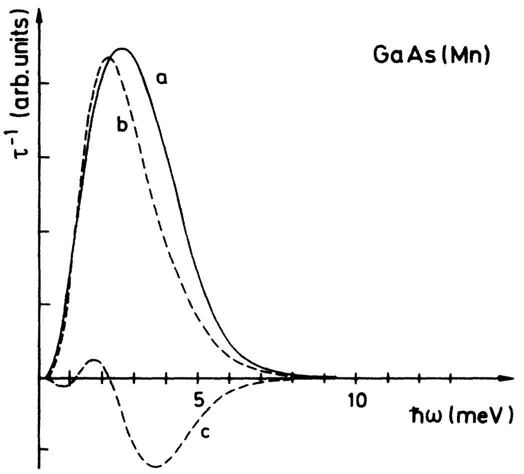

FIG. 1. Relaxation rate in the case of GaAs(Mn): curve a is the total relaxation rate due to Eq. (50); curve b the first part of Eq. (50); curve c the second part of Eq. (50).

As we have expected Eq. (50) shows a resonancelike structure.[19,20] Δ and Γ, however, are frequency dependent. A resonance frequency may be defined if we demand

$$\omega_{\text{res}}^2-\Delta(\omega_{\text{res}})=0\ . \tag{55}$$

This frequency is for all considered systems very close to $\omega_{\max}$, the frequency of maximum scattering rate. This can be seen in Fig. 1 where the relaxation rate and the real and imaginary parts are plotted against the frequency.

Our final results for the Green function fulfills the sum rules (26) and (27) as well as the symmetry relation (25) contrary to former calculations done for these systems.[10]

VII. COMPARISON WITH PERTURBATION THEORY

Comparing our theory with perturbational approaches,[9] the results are the same in the limit of small coupling parameters ($D_\epsilon, D_\tau \rightarrow 0$) as shown in an earlier paper concerning the thermal conductivity.[6] A resonance structure as we found, however, cannot be predicted by the perturbational treatment.

In the limit of small frequencies $\omega\rightarrow0$ a different behavior from the perturbational one is predicted. In this limiting case expression (50) reduces to a ω^4 law,

$$\langle\tau^{-1}(\omega)\rangle=\frac{8}{9}D_\epsilon^2\frac{\hbar\omega n\pi}{\rho\bar{c}^{\,2}}\frac{1}{9}\sum_{\lambda=1}^{3}f_\lambda^2(\omega)\frac{\beta(\omega)}{\Delta_3+\Delta_5+\Delta_6}\ , \tag{56}$$

in contrast to the perturbational result which gives a ω^2 dependence[9]

$$\langle\tau_\lambda^{-1}(\omega)\rangle=\frac{n}{100\pi}\frac{\omega^2}{\rho^2\hbar^2c_\lambda^2}(\tfrac{2}{3}D_\tau)^4f_\lambda^2(\omega)$$

$$\times\left[\frac{1}{c_l^5}f_l^2(\omega)+\frac{3}{2}\frac{1}{c_t^5}f_t^2(\omega)\right]W_\lambda\ , \tag{57}$$

with

$$W_1=4+48D^2+8D^4\ ,$$

$$W_2=16+37D^2+7D^4\ ,$$

$$W_3=20+35D^2+5D^4\ .$$

The reason for this different frequency behavior lies in the dynamically induced splitting terms arising from the RPA. In the perturbation theory an analogous static splitting is absent due to the degeneracy of the electronic ground state. Further on in this case ($\omega\rightarrow0$) the validity of the perturbation theory is questionable due to the $\omega^{-1/2}$ dependence of the dimensionless coupling constant. This difference between both methods in the low-frequency limit, however, exists for the case of an electronically degenerate ground state only. The introduction of static splittings immediately changes the perturbational result to a ω^2 dependence, too.

The main difference between the outlined theory and the usual perturbational approaches, however, lies in the fact that for the considered systems (i) a resonance structure for the scattering rate cannot be predicted by the perturbational treatment, and (ii) the temperature dependence of the results of both methods are totally different as will be discussed later.

VIII. DEPENDENCE ON PHYSICAL PARAMETERS

We used Eq. (50) to determine the resonance behavior of different acceptor systems, e.g., Si(B), Si(In), and GaAs(Mn). The physical parameters needed in the theory are given in Table I. They are all well defined and there is no adjustable parameter. The Bohr radii, however, are not very well known from experiment. Nevertheless all parameters are determined by independent experiments. The used values of the deformation potential constants are calculated from the measured ones by taking the reduction due to the Jahn-Teller interaction into account.[19] In Table II the calculated unreduced values are given.

Before comparing the calculated resonance energies with experimental values we will focus on measurements done several years ago by Schad.[22] For the discussed acceptor systems he claimed for the resonance frequency the experimentally found relation

$$\omega_{\mathrm{res}} \sim \frac{\bar{\epsilon}}{a^*} , \tag{58}$$

whereby the dependence on the static dielectricity constant $\bar{\epsilon}$ by considering only two different physical systems (GaAs and Si) is not convincing.

To determine the resonance frequency we have to discuss expression (50). This frequency is given when expression (50) reaches it maximum value. The numerical calculations show that for all acceptor systems $\Delta(\omega) >> \omega$, except at a very narrow range around the resonance frequency. This fact enables us to look for a more simplified expression for the resonance frequency than that given by (50), namely, it may be determined by the sign change of $\Delta(\omega)$. This change is caused by the frequency-dependent integrals S^λ and $\tilde{S}^\lambda$. In all considered systems the term Δ_2 dominates and therefore the following relation holds for ω_{res}:

$$S^\lambda(\omega_{\mathrm{res}},2)=0 . \tag{59}$$

TABLE I. System parameters of the semiconductor crystals considered in the paper.

	GaAs	Si
Atomic weight	72.3	28.1
ω_D (MeV)	29.76	56.77
ρ (kg/m^3)	5.3×10^3	2.33×10^3
c_l (m/sec)	5.21×10^3	9.1×10^3
c_t (m/sec)	3.0×10^3	4.55×10^3

TABLE II. Defect properties for several acceptor types.

	GaAs(Mn)	Si(In)	Si(B)	Si(Al)	Si(Ga)
$\tilde{D}_\epsilon$ (eV)	0.53	1.47	2.13	2.15	~2
$\tilde{D}_\tau$ (eV)	0.69	2.32	3.20	3.33	~2
a^* (Å)	6	7.3	13.6	10.9	10.6

Due to the cutoff the assumption $\omega_D \rightarrow \infty$ is physically reasonable and therefore in this case expression (59) can be evaluated to give $[d_\lambda=(a^*/2c_\lambda)^2]$

$$-\frac{5}{16}+\frac{5}{16}\frac{d_\lambda\omega^2}{(1+d_\lambda\omega^2)}+\frac{3}{8}\frac{d_\lambda\omega^2}{(1+d_\lambda\omega^2)^2}+\frac{1}{2}\frac{d_\lambda\omega^2}{(1+d_\lambda\omega^2)^3}+\frac{d_\lambda\omega^2}{(1+d_\lambda\omega^2)^4}=0 . \tag{60}$$

The only variable which appears is $(d_\lambda)^{1/2}\omega=(a^*/2c_\lambda)\omega$, and $(1+d_\lambda\omega^2)$ can be approximated by 1 and therefore for the solution of (60) one gets

$$\omega_{\mathrm{res}} \sim \frac{1}{a^*} . \tag{61}$$

This means we get the same Bohr radius dependence as Schad deduced from the experiments.

In the cases of acceptors the solutions of (60) and the resonance frequency calculated directly from expression (50) are nearly identical. The results compared with experimental values are given in Table III. The theory, which contains no fit parameter, reproduce the experimental values quite well. For the hypothetical case of vanishing Bohr radius the frequency integrations can only be evaluated up to the Debye frequency ω_D. In this case from (60) we get

$$\omega_{\mathrm{res}}=0.83\omega_D . \tag{62}$$

One sees that even in this limiting case the resonance character of the scattering rate is preserved in contrast to the perturbational result (57).

Figure 2 shows the relaxation rate for Si(In) together with the perturbational result and the weak coupling limit approximation. The second (small) maximum at approximately $2\omega_{\mathrm{res}}$ appearing in the result of our theory is due to the high-order calculations and gives two-phonon contributions which, however, are strongly suppressed by the cutoff function. Figure 3 shows the relaxtion rate for GaAs(Mn) where no such additional peak appears.

As mentioned before the most striking difference be-

TABLE III. Values of the resonances energies of the considered acceptor systems. The parameters used for the calculation are given in Tables I and II.

	GaAs(Mn)	Si(In)	Si(B)
Experimental values (meV)	3.1 ± 0.3	4.2 ± 0.2	2
References	21,2	5	3
Calculated form the change of sign of $S^\lambda(\omega,2)$	2.7	4.4	2.3

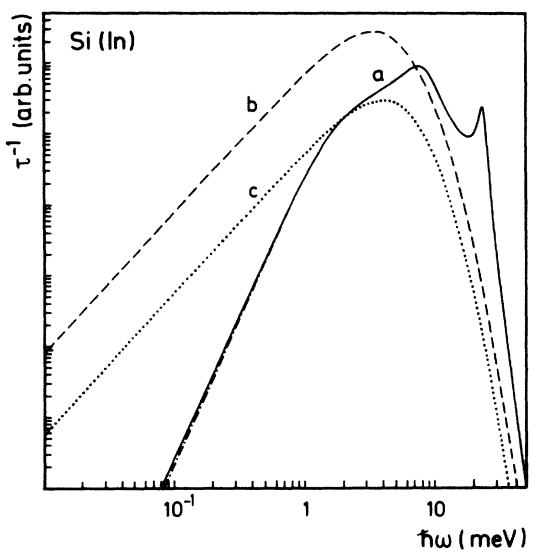

FIG. 2. Relaxation rate in the case of Si(In): curve a is the total relaxation rate due to Eq. (50); curve b the perturbation theory (Ref. 9); curve c the approximation of Eq. (50) for small D_ϵ, D_T.

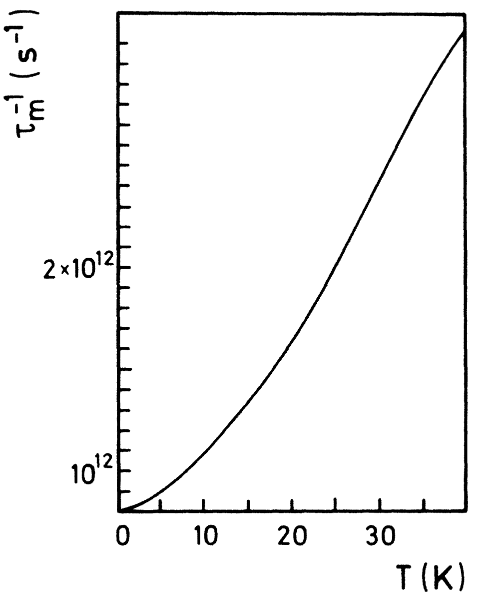

FIG. 4. Temperature dependence of the maximum scattering rate.

tween the perturbational result (57) and our theory (50) lies in the temperature dependence which is completely absent in perturbation theory whereas in the Green-function approach the maximum scattering rate as well as the linewidth are strongly temperature dependent. This is physically reasonable from the coupling of all phonons of the crystal which act as a heat bath. In the case of GaAs(Mn) this temperature dependence is shown in Fig. 4. The influence of temperature on linewidth and resonance frequency is plotted in Fig. 5. There is no obvious trend for the resonance frequency but the linewidth shows a maximum at some 20 K where the resonances in thermal conductivity are observed.[6]

In Fig. 6 resonance energy and half-width of the resonance curve are drawn against the Bohr radius with the other parameters of Si(In) fixed. The resonance energy shows the behavior of Eq. (61) whereas the half-width

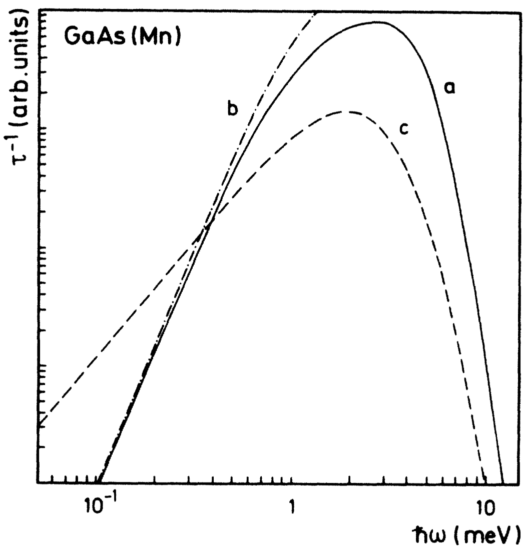

FIG. 3. Relaxation rate in the case of GaAs(Mn): curve a is the total relaxation rate due to Eq. (50); curve b the approximation of Eq. (50) for small ω's; curve c the approximation of Eq. (50) for small D_ϵ, D_T.

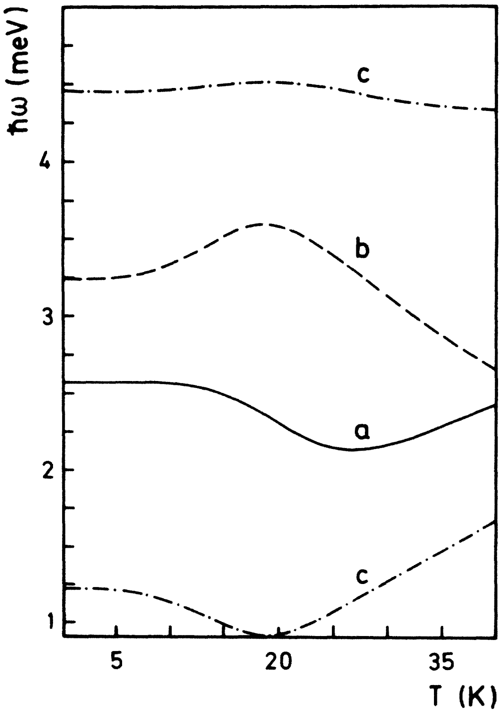

FIG. 5. Temperature dependence of the resonance frequency and linewidth: curve a is the resonance frequency; curve b the linewidth; curve c the energy values, where the scattering rate is half of the maximum value.

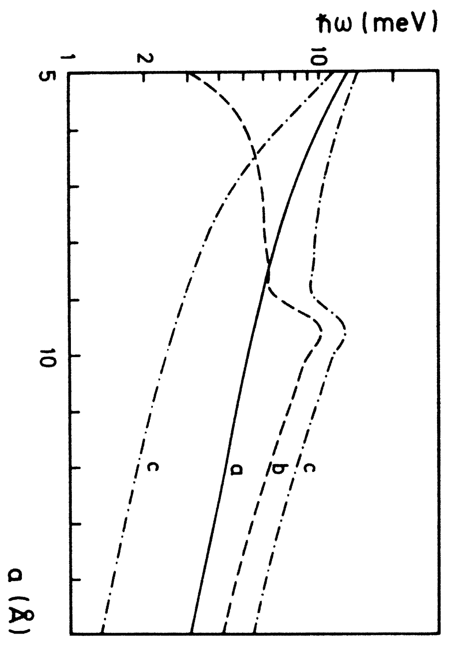

FIG. 6. Bohr radius dependence of the frequency and linewidth: curve a is the resonance frequency; curve b the linewidth; curve c the energy values, where the scattering rate is half of the maximum value.

changes at about 10 meV. This is due to the change in the line shape also visible in the comparison of Figs. 2 and 3.

IX. CONCLUSIONS

In this paper we investigated a specific resonance mechanism which is due to the dynamic interaction between electronic states and phonons and therefore of nonadiabatic origin. We concentrated our calculations on acceptor defects in cubic semiconductors where these resonance structures were detected for the first time in thermal conductivity measurements.[2,23] Nevertheless, the requirements for this type of resonances, i.e., a defect with a weak JT interaction should also be present in other systems.

As we have shown the described phonon scattering mechanism cannot be treated by usual perturbation theory, it requires a higher-order calculation to include the influence of all the coupled phonon modes. It is just this influence which leads to a very broad and strongly temperature-dependent scattering rate. This behavior of the scattering rate on the other hand is responsible for the strong influence on thermal conductivity which even can lead to a minimum in the conductivity curves.[2,6] In a forthcoming paper we plan to study the influence of elastic and magnetic fields on the behavior of the systems and show how these special dynamics can be destroyed by applying static fields to the defects.

ACKNOWLEDGMENTS

The authors gratefully acknowledge financial support by a grant of Deutsche Forschungsgemeinschaft (DFG). They would like to thank L. Challis, A. M. de Goer, and K. Lassmann for numerous discussions on this subject.

APPENDIX A: SU(4) OPERATORS

The commutation relations between the SU(4) operators as well as the definitions of the operators ξ_i

TABLE IV. Commutation relations betweeen the SU(4) operators and definitions of the operators ξ_i $(i=1,\ldots,15)$. The values in the table have to be multiplied by $2i$.

	ρ_1	ρ_2	$\rho_3\sigma_1$	$\rho_3\sigma_2$	$\rho_3\sigma_3$	ρ_3	$\rho_1\sigma_1$	$\rho_1\sigma_2$	$\rho_1\sigma_3$	$\rho_2\sigma_1$	$\rho_2\sigma_2$	$\rho_2\sigma_3$	σ_1	σ_2	σ_3
$\rho_1\simeq\xi_1$		ρ_3	$-\rho_2\sigma_1$	$-\rho_2\sigma_2$	$-\rho_2\sigma_3$	$-\rho_2$				$\rho_3\sigma_1$	$\rho_3\sigma_2$	$\rho_3\sigma_3$			
$\rho_2\simeq\xi_2$	$-\rho_3$		$\rho_1\sigma_1$	$\rho_1\sigma_2$	$\rho_1\sigma_3$	ρ_1	$-\rho_3\sigma_1$	$-\rho_3\sigma_2$	$-\rho_3\sigma_3$						
$\rho_3\sigma_1\simeq\xi_3$	$\rho_2\sigma_1$	$-\rho_1\sigma_1$		σ_3	$-\sigma_2$		ρ_2			$-\rho_1$				$\rho_3\sigma_3$	$-\rho_3\sigma_2$
$\rho_3\sigma_2\simeq\xi_4$	$\rho_2\sigma_2$	$-\rho_1\sigma_2$	$-\sigma_3$		σ_1			ρ_2			$-\rho_1$		$-\rho_3\sigma_3$		$\rho_3\sigma_1$
$\rho_3\sigma_3\simeq\xi_5$	$\rho_2\sigma_3$	$-\rho_1\sigma_3$	σ_2	$-\sigma_1$					ρ_2			$-\rho_1$	$\rho_3\sigma_2$	$-\rho_3\sigma_1$	
$\rho_3\simeq\xi_6$	ρ_2	$-\rho_1$					$\rho_2\sigma_1$	$\rho_2\sigma_2$	$\rho_2\sigma_3$	$-\rho_1\sigma_1$	$-\rho_1\sigma_2$	$-\rho_1\sigma_3$			
$\rho_1\sigma_1\simeq\xi_7$		$\rho_3\sigma_1$	$-\rho_2$			$-\rho_2\sigma_1$		σ_3	$-\sigma_2$	ρ_3				$\rho_1\sigma_3$	$-\rho_1\sigma_2$
$\rho_1\sigma_2\simeq\xi_8$		$\rho_3\sigma_2$		$-\rho_2$		$-\rho_2\sigma_2$	$-\sigma_3$		σ_1		ρ_3		$-\rho_1\sigma_3$		$\rho_1\sigma_1$
$\rho_1\sigma_3\simeq\xi_9$		$\rho_3\sigma_3$			$-\rho_2$	$-\rho_2\sigma_3$	σ_2	$-\sigma_1$				ρ_3	$\rho_1\sigma_2$	$-\rho_1\sigma_1$	
$\rho_2\sigma_1\simeq\xi_{10}$	$-\rho_3\sigma_1$		ρ_1			$\rho_1\sigma_1$	$-\rho_3$				σ_3	$-\sigma_2$		$\rho_2\sigma_3$	$-\rho_2\sigma_2$
$\rho_2\sigma_2\simeq\xi_{11}$	$-\rho_3\sigma_2$			ρ_1		$\rho_1\sigma_2$		$-\rho_3$		$-\sigma_3$		σ_1	$-\rho_2\sigma_3$		$\rho_2\sigma_1$
$\rho_2\sigma_3\simeq\xi_{12}$	$-\rho_3\sigma_3$				ρ_1	$\rho_1\sigma_3$			$-\rho_3$	σ_2	$-\sigma_1$		$\rho_2\sigma_2$	$-\rho_2\sigma_1$	
$\sigma_1\simeq\xi_{13}$				$\rho_3\sigma_3$	$-\rho_3\sigma_2$			$\rho_1\sigma_3$	$-\rho_1\sigma_2$		$\rho_2\sigma_3$	$-\rho_2\sigma_2$		σ_3	$-\sigma_2$
$\sigma_2\simeq\xi_{14}$			$-\rho_3\sigma_3$		$\rho_3\sigma_1$		$-\rho_1\sigma_3$		$\rho_1\sigma_1$	$-\rho_2\sigma_3$		$\rho_2\sigma_1$	$-\sigma_3$		σ_1
$\sigma_3\simeq\xi_{15}$			$\rho_3\sigma_2$	$-\rho_3\sigma_1$			$\rho_1\sigma_2$	$-\rho_1\sigma_1$		$\rho_2\sigma_2$	$-\rho_2\sigma_1$		σ_2	$-\sigma_1$	

$(i=1,2,\ldots,15)$ are given in Table IV. The SU(4) operators can be expressed in Fermi creation and annihilation operators $c_i^\dagger$, c_i $(i=1,2,3,4)$ of the electronic Γ_8 state

$$\rho_1=(c_1^\dagger c_3+c_3^\dagger c_1)+(c_2^\dagger c_4+c_4^\dagger c_2)\ ,$$

$$\rho_2=i(c_3^\dagger c_1-c_1^\dagger c_3)+i(c_4^\dagger c_2-c_2^\dagger c_4)\ ,$$

$$\rho_3=c_1^\dagger c_1+c_2^\dagger c_2-c_3^\dagger c_3-c_4^\dagger c_4\ ,$$

$$\sigma_1=(c_1^\dagger c_2+c_2^\dagger c_1)+(c_3^\dagger c_4+c_4^\dagger c_3)\ ,$$

$$\sigma_2=i(c_2^\dagger c_1-c_1^\dagger c_2)+i(c_4^\dagger c_3-c_3^\dagger c_4)\ ,$$

$$\sigma_3=c_1^\dagger c_1-c_2^\dagger c_2+c_3^\dagger c_3-c_4^\dagger c_4\ ,$$

$$\rho_1\sigma_1=(c_1^\dagger c_4+c_4^\dagger c_1)+(c_2^\dagger c_3+c_3^\dagger c_2)\ ,$$

$$\rho_1\sigma_2=i(c_4^\dagger c_1-c_1^\dagger c_4)+i(c_2^\dagger c_3-c_3^\dagger c_2)\ ,$$

$$\rho_1\sigma_3=(c_1^\dagger c_3+c_3^\dagger c_1)-(c_2^\dagger c_4+c_4^\dagger c_2)\ ,$$

$$\rho_2\sigma_1=i(c_4^\dagger c_1-c_1^\dagger c_4)+i(c_3^\dagger c_2-c_2^\dagger c_3)\ ,$$

$$\rho_2\sigma_2=-(c_1^\dagger c_4+c_4^\dagger c_1)+(c_2^\dagger c_3+c_3^\dagger c_2)\ ,$$

$$\rho_2\sigma_3=i(c_3^\dagger c_1-c_1^\dagger c_3)+i(c_2^\dagger c_4-c_4^\dagger c_2)\ ,$$

$$\rho_3\sigma_1=(c_1^\dagger c_2+c_2^\dagger c_1)-(c_3^\dagger c_4+c_4^\dagger c_3)\ ,$$

$$\rho_3\sigma_2=i(c_2^\dagger c_1-c_1^\dagger c_2)+i(c_3^\dagger c_4-c_4^\dagger c_3)\ ,$$

$$\rho_3\sigma_3=c_1^\dagger c_1-c_2^\dagger c_2-c_3^\dagger c_3+c_4^\dagger c_4\ .$$

TABLE V. Angle-dependent integrations. j denotes the phonon type, j is the branch index.

	$\lambda=1$	$\lambda=2$	$\lambda=3$
$j=1$	$\frac{16}{45}\pi D_\epsilon^2$	$\frac{8}{15}\pi D_\epsilon^2$	0
$j=2$	$\frac{16}{45}\pi D_\epsilon^2$	$\frac{4}{45}\pi D_\epsilon^2$	$\frac{4}{9}\pi D_\epsilon^2$
$j=3$	$\frac{16}{45}\pi D_\tau^2$	$\frac{16}{45}\pi D_\tau^2$	$\frac{2}{9}\pi D_\tau^2$
$j=4$	$\frac{16}{45}\pi D_\tau^2$	$\frac{16}{45}\pi D_\tau^2$	$\frac{2}{9}\pi D_\tau^2$
$j=5$	$\frac{16}{45}\pi D_\tau^2$	$\frac{4}{45}\pi D_\tau^2$	$\frac{4}{9}\pi D_\tau^2$

APPENDIX B: DEFINITION OF THE FUNCTIONS A_j^λ AS RESULT OF THE ANGLE INTEGRATION

All angle-dependent integrations appearing by converting sums into integrals can be solved analytically. The results are given in Table V.

APPENDIX C: CALCULATION OF THE INTEGRALS FOR THE RELAXATION RATE EQUATIONS (49a)–(49d)

Restricting ourselves to the simple Lorentzian form of the cutoff function, i.e. $[d_\lambda=(a^*/2c_\lambda)^2]$,

$$f_\lambda(\omega_{q\lambda})=(1+d_\lambda\omega_{q\lambda}^2)^{-2}\ ,$$

the temperature-independent integrals result in rational functions. So they may be easily solved.[24]

The following equation is needed for the solutions

$$\frac{1}{(x^2-a^2)(1+dx^2)^4}=\frac{d}{1+da^2}\left[\frac{1}{(1+dx^2)^4}+\frac{1}{(1+da^2)}\frac{1}{(1+dx^2)^3}-\frac{1}{(1+da^2)^2}\frac{1}{(1+dx^2)^2}+\frac{1}{(1+da^2)^3}\frac{1}{(1+dx^2)}\right]+\frac{1}{(1+da^2)^4}\frac{1}{x^2-a^2}\ .$$

The calculation of the various integrals is done with the following recurrence relations:

$$\int_0^{\omega_D}d\omega\frac{\omega^n}{\omega^2-a^2}=-\left.\frac{\omega^{n-1}}{n-1}\right|_0^{\omega_D}+a^2\int_0^{\omega_D}d\omega\frac{\omega^{n-2}}{\omega^2-a^2}\quad\text{for } n\geq 2\ ,$$

$$\int d\omega\frac{1}{\omega^2-a^2}=\frac{1}{2a}\ln\left|\frac{\omega+a}{\omega-a}\right|\ ,$$

$$\int d\omega\frac{\omega}{\omega^2-a^2}=\tfrac{1}{2}\ln|\omega^2-a^2|\ ,$$

$$\int d\omega\frac{1}{(1+d\omega^2)}=\frac{1}{\sqrt{d}}\arctan(\omega\sqrt{d}\,)\ ,$$

$$\int_0^{\omega_D}\int d\omega\frac{\omega^m}{(1+d\omega^2)^n}=\begin{cases}\dfrac{1}{d}\displaystyle\int_0^{\omega_D}d\omega\frac{\omega^{m-2}}{(1+d\omega^2)^{n-1}}-\frac{1}{d}\int_0^{\omega_D}d\omega\frac{\omega^{m-2}}{(1+d\omega^2)^n} & \text{for } n=2m-1,\\[2ex] \dfrac{m-1}{d(2n-m-1)}\displaystyle\int_0^{\omega_D}d\omega\frac{\omega^{m-2}}{(1+d\omega^2)^n}-\left.\frac{\omega^{m-1}}{(1+d\omega^2)^{n-1}}\right|_0^{\omega_D} & \text{for } n\neq 2m-1\ .\end{cases}$$

The calculation of the temperature-dependent integrals cannot be done analytically. A numerical integration is impossible due to CPU time considerations. We therefore developed the coth part[25]

$$\coth x = \frac{1}{x} + \sum_{k=1}^{\infty} \frac{2^{2k} B_{2k}}{(2k)!} x^{2k-1} ,$$

where B_n are Bernoulli's numbers.

This series converges for $|x| < \pi$. Even for $k < 5$ good results are received in accordance with numerical calculations. Together with this series no new type of integrals is needed, therefore this method was chosen despite other methods with better convergence conditions.[25] All the integrals are of Cauchy principal-value type.

---

[*] Present address: Robert Bosch GmbH, Abteilung Forschung Physik und Technologie, D-7000 Stuttgart, Federal Republic of Germany.

[1] W. E. Bron, Rep. Prog. Phys. **43**, 301 (1980).

[2] A. de Combarieu and K. Lassmann, in *Phonon Scattering in Solids,* edited by L. J. Challis, V. W. Rampton, and A. F. G. Wyatt (Plenum, New York, 1976).

[3] A. Ambrosy, A. M. de Goer, K. Lassmann, B. Salce, and H. Zeile, *Phonon Scattering in Solids* (Springer, Berlin, 1984).

[4] P. Tuerkes, Ph.D. thesis, University of Erlangen, 1983 (unpublished).

[5] K. Lassmann and Hp. Schad, Solid State Commun. **18**, 449 (1976).

[6] J. Maier and E. Sigmund, J. Phys. C **17**, 4141 (1984).

[7] M. Rueff, E. Sigmund, and M. Wagner, Phys. Status Solidi B **81**, 511 (1977).

[8] T. N. Morgan, Phys. Rev. Lett. **24**, 887 (1970).

[9] K. Suzuki and N. Mikoshiba, Phys. Rev. B **3**, 2550 (1971).

[10] E. Sigmund and K. Lassmann, Phys. Status Solidi B **111**, 631 (1982).

[11] A. Puhl, E. Sigmund, and J. Maier, Phys. Rev. B **32**, 8234 (1985).

[12] S. Schweber, *An Introduction to Relativistic Quantum Field Theory* (Harper&Row, New York, 1961).

[13] R. Levine, *Quantum Mechanics of Molecular Rate Processes,* (Clarendon, Oxford, 1969).

[14] K. Elk and W. Gasser, *Die Methode der Greenschen Funktionen in der Festkörperphysik* (Akademie Verlag, Berlin, 1979).

[15] H. J. Lipkin, in *Anwendung Liescher Gruppen in der Physik,* (Hochschultaschenbücher, Mannheim, 1967).

[16] D. Schechter, J. Phys. Chem. Solids **3**, 237 (1962).

[17] M. V. Klein, Phys. Rev. **131**, 1500 (1963).

[18] M. V. Klein, Phys. Rev. **186**, 839 (1969).

[19] E. Sigmund and J. Maier, in *Proceedings of the International Symposium on Synergetics and Cooperative Phenomena in Solids and Macromolecules,* edited by A. Sherman (Acad. of Sciences, Estonian SSR, 1982).

[20] J. Maier and E. Sigmund, J. Phys. (Paris) Colloq. **C6-42**, 232 (1981).

[21] J. Maier and E. Sigmund, Solid State Commun. **51**, 961 (1984).

[22] Hp. Schad, Ph.D. thesis, University of Stuttgart, 1976 (unpublished).

[23] M. G. Holland, Seventh International Conference on Semiconductors, Paris, 1964 (unpublished).

[24] I. N. Bronstein and K. A. Semendjajew, *Taschenbuch der Mathematik* (Teubner, Leipzig, 1974).

[25] M. Abramowitz and I. A. Stegun, *Handbook of Mathematical Functions* (Academic, New York, 1972).